BBA - Molecular Basis of Disease 1865 (2019) 165530

Contents lists available at ScienceDirect

BBA - Molecular Basis of Disease

journal homepage: www.elsevier.com/locate/bbadis

Simvastatin induces autophagic flux to restore cerulein-impaired phagosome-lysosome fusion in acute pancreatitis

Honit Piplani[a,b], Stefanie Marek-Iannucci[a,b], Jon Sin[a,b], Jean Hou[c], Toshimasa Takahashi[d], Ankush Sharma[e], Juliana de Freitas Germano[a,b], Richard T. Waldron[b], Hannaneh Saadaeijahromi[a,b], Yang Song[a,b], Aiste Gulla[f,g], Bechien Wu[h], Aurelia Lugea[b], Allen M. Andres[a,b], Herbert Y. Gaisano[d], Roberta A. Gottlieb[a,b,*], Stephen J. Pandol[b,**]

[a] Smidt Heart Institute, Cedars-Sinai Medical Center, Los Angeles, CA, USA
[b] Department of Medicine, Cedars-Sinai Medical Center, Los Angeles, CA, USA
[c] Department of Pathology, Cedars-Sinai Medical Center, Los Angeles, CA, USA
[d] Department of Medicine, University of Toronto, Toronto, Ontario M5S1A8, Canada
[e] Institute of Biosciences and Department of Informatics, University of Oslo, Norway
[f] Department of Surgery, MedStar Georgetown University Hospital, USA
[g] Vilnius University Hospital Santaros Klinikos, Lithuania
[h] Kaiser Permanente Los Angeles Medical Center, Los Angeles, CA, USA

ARTICLE INFO

Keywords:
Simvastatin
Mitochondria
Pancreatitis
Autophagic flux
Parkin

ABSTRACT

Background: During pancreatitis, autophagy is activated, but lysosomal degradation of dysfunctional organelles including mitochondria is impaired, resulting in acinar cell death. Retrospective cohort analyses demonstrated an association between simvastatin use and decreased acute pancreatitis incidence.

Methods: We examined whether simvastatin can protect cell death induced by cerulein and the mechanisms involved during acute pancreatitis. Mice were pretreated with DMSO or simvastatin (20 mg/kg) for 24 h followed by 7 hourly cerulein injections and sacrificed 1 h after last injection to harvest blood and tissue for analysis.

Results: Pancreatic histopathology revealed that simvastatin reduced necrotic cell death, inflammatory cell infiltration and edema. We found that cerulein triggered mitophagy with autophagosome formation in acinar cells. However, autophagosome-lysosome fusion was impaired due to altered levels of LAMP-1, AMPK and ULK-1, resulting in autophagosome accumulation (incomplete autophagy). Simvastatin abrogated these effects by upregulating LAMP-1 and activating AMPK which phosphorylated ULK-1, resulting in increased formation of functional autolysosomes. In contrast, autophagosomes accumulated in control group during pancreatitis. The effects of simvastatin to promote autophagic flux were inhibited by chloroquine. Mitochondria from simvastatin-treated mice were resistant to calcium overload compared to control, suggesting that simvastatin induced mitochondrial quality control to eliminate susceptible mitochondria. Clinical specimens showed a significant increase in cell-free mtDNA in plasma during pancreatitis compared to normal controls. Furthermore, genetic deletion of parkin abrogated the benefits of simvastatin.

Conclusion: Our findings reveal the novel role of simvastatin in enhancing autophagic flux to prevent pancreatic cell injury and pancreatitis.

Abbreviations: AMPK, 5′ AMP-activated protein kinase; ATP, Adenosine triphosphate; ATP5A, ATP synthase F1 subunit alpha; GFP, Green fluorescent protein; LAMP, Lysosome-associated membrane glycoprotein; Mfn2, Mitofusin 2; MMP, Mitochondrial membrane permeabilization; MTCO1, Mitochondria-encoded cytochrome *c* oxidase I; mtDNA, Mitochondrial DNA; NDUFB8, NADH:Ubiquinone oxidoreductase subunit B8; NLRP3, Nucleotide-binding oligomerization family pyrin domain containing 3; OXPHOS, Oxidative phosphorylation; ROS, Reactive oxygen species; SDHB, Succinate dehydrogenase complex iron sulfur subunit B; Simva, Simvastatin; SNARE, Soluble N-ethylmaleimide-sensitive factor protein receptor; Stx17, Syntaxin 17; TFAM, Transcription factor A, mitochondrial; TLR9, Toll-like receptor 9; TUNEL, Terminal deoxynucleotidyl transferase dUTP nick end labeling; ULK1, Unc-51 like autophagy activating kinase 1; UQCRC2, Ubiquinol-cytochrome C reductase core protein 2

* Correspondence to: R.A. Gottlieb, Smidt Heart Institute, Cedars-Sinai Medical Center, Los Angeles, CA, USA.
** Corresponding author.
E-mail addresses: roberta.gottlieb@cshs.org (R.A. Gottlieb), stephen.pandol@cshs.org (S.J. Pandol).

https://doi.org/10.1016/j.bbadis.2019.08.006
Received 24 December 2018; Received in revised form 16 July 2019; Accepted 5 August 2019
Available online 06 August 2019
0925-4439/

1. Introduction

Acinar cell injury regulates the severity of acute pancreatitis by activating downstream signaling cascades including release of inflammatory mediators and recruitment of inflammatory cells [1,2]. Intracellular events in pancreatitis begin with Ca^{2+} release from endoplasmic reticulum stores promoting extracellular Ca^{2+} influx into the acinar cell via store-operated plasma membrane channels, leading to excessive uptake by mitochondria [3,4]. The sustained mitochondrial calcium overload during pancreatitis results in mitochondrial membrane permeabilization (MMP). Damaged mitochondria can produce excessive reactive oxygen species (ROS), resulting in oxidative modification of mitochondrial proteins and mitochondrial DNA (mtDNA), further compounding mitochondrial dysfunction [5,6], and leading to defective autophagy, zymogen activation, inflammation, and necrosis [3].

Autophagy is the process of removal of damaged cellular components including dysfunctional mitochondria (mitophagy) during stress conditions [7]. Hashimoto D et al. (2008) showed the involvement of autophagy and accumulation of autophagic vacuoles during acute pancreatitis [8]. LC3, a product of *MAP1LC3A* gene, is a vital protein required for phagophore elongation after it is lipidated (designated LC3-II), which anchors it to the autophagosomal membrane. LC3 lipidation occurs during pancreatitis [9,10]. The pancreas has a high rate of basal autophagy compared to other organs [11,12]; however, during pancreatitis, fusion of autophagosomes with lysosomes and the subsequent digestion of cargo is impaired despite elevated autophagosome initiation [13]. This leads to accumulation of autophagosomes containing dysfunctional mitochondria and zymogen granules [10]; breakdown or extracellular release of autophagosomes results in release of oxidized mtDNA which can contribute to acinar cell damage. Mitophagy is a protective mechanism invoked during various cellular stresses[1]. Removal of damaged mitochondria by mitophagy, followed by replacement mitochondrial biogenesis serves to maintain mitochondrial bioenergetics for efficient Adenosine triphosphate (ATP) production [14]. Mitophagy occurs through parkin-dependent and -independent mechanisms [15]. Parkin is an evolutionarily conserved E3 ubiquitin ligase encoded by the *Park2* gene [16] which poly-ubiquitinates multiple targets on the mitochondrial outer membrane, thereby recruiting p62/SQSTM1 to depolarized mitochondria. P62 binds ubiquitinated proteins and recruits an LC3-decorated phagophore to engulf the ubiquitinated mitochondrion [17]. Autophagosomes containing their cargo are transported along microtubules and aggregate in the perinuclear region [18]. Autophagosomes eventually fuse with lysosomes, resulting in degradation of the cargo including mitochondria and zymogen granules. Recently, syntaxin 17 emerged as an important participant in the fusion process which requires lysosome-associated membrane glycoproteins (LAMPs) [19]. LAMPs maintain pancreatic acinar cell homeostasis and their deletion is known to cause pancreatitis [20]. Delivery of mitochondria to lysosomes also requires the activity of AMP activated protein kinase (AMPK) to phosphorylate Unc-51 like autophagy activating kinase 1 (ULK1) [21], inducing both autophagy and mitophagy [22,23]. Mitophagy is closely linked to mitochondrial biogenesis to maintain proper mitochondrial homeostasis, and we recently showed that mitochondrial biogenesis occurs rapidly along with mitophagy during cardiopulmonary bypass [24,25]. However, there is no knowledge about the potential role of mitochondrial turnover through mitophagy and mitochondrial biogenesis in pancreatitis.

Retrospective cohort analyses have demonstrated an association between simvastatin use (and potentially other statin use) and decreased pancreatitis incidence as well as recurrence of pancreatic cancer after surgery [26,27]. Statins are inhibitors of 3-hydroxy-3-methylglutaryl coenzyme A (HMG-CoA) reductase which is the rate limiting enzyme in cholesterol biosynthesis and has been demonstrated to have protective effects in cardiac ischemia/reperfusion experiments, even when given within a few hours before the insult [28]. We further showed that simvastatin can induce mitophagy in cardiac cells, mitigating the ischemic injury due in part to a stress-resistant mitochondrial population [28]. Pancreatitis has many similarities to cardiac ischemia/reperfusion, with the calcium influx and damaging effects of inflammatory cells mimicking the events of reperfusion.

This study sought to elucidate the role of simvastatin in preventing the cellular injury during pancreatitis. Enhanced autophagic flux have been determined to play a vital role in the protective effects of simvastatin, which also decreased the infiltration of inflammatory cells, reduced the accumulation of vacuoles, release of mtDNA, and necrotic cell death. Using an in vivo mouse model of acute pancreatitis, we have shown that simvastatin has a protective effect in attenuating pancreatitis responses and that the effect of simvastatin in the pancreas is parkin dependent.

2. Methods

2.1. Clinical samples

Clinical plasma samples were obtained from a previous study conducted at the Department of Surgery at Kaunas University of Medicine Hospital (Lithuania). Patients admitted during 2006–2007 with a diagnosis of alcoholic pancreatitis, history of significant alcohol intake and onset of the acute illness within the preceding 72 h were included in this study. Plasma samples from healthy controls were obtained during the same dates (2006–2007) by the medical team using similar procedures used in patients. The samples were frozen at −80 °C and shipped on dry ice. The Regional Ethics Committee approved the study (protocols No. BE-2-47 and P1-113/2005) and all the patients and healthy controls provided written informed consent. The diagnosis was established on the basis of acute abdominal pain and at least 3-fold elevated levels of serum amylase or typical radiological findings of acute pancreatitis. Patients with underlying chronic pancreatitis and patients with acute pancreatitis referred to the hospital from other institutions after management for > 3 d were excluded from this study.

2.2. Animal ethics

All animal procedures followed the National Institute of Health standards and were approved by the Institutional Animal Care and Use Committee of Cedars-Sinai Medical Center.

2.3. Animal model of acute pancreatitis

C57BL/6 male mice (8–12 weeks age) were pretreated with intraperitoneal (i.p.) injection of DMSO (50 μl) or simvastatin (20 mg/kg b.w. dissolved in DMSO) for 24 h prior to 7-hourly i.p. injections of cerulein (50 μg/kg), a CCK analog used for experimental pancreatitis models. Control animals received the same amount of saline injections. Animals were sacrificed using cervical dislocation method after 60 min of last injection (Supplementary Fig. 1). Blood and pancreatic tissue were obtained and processed for different measurements.

2.4. Histology

H&E staining was performed on pancreata as described in supplementary information.

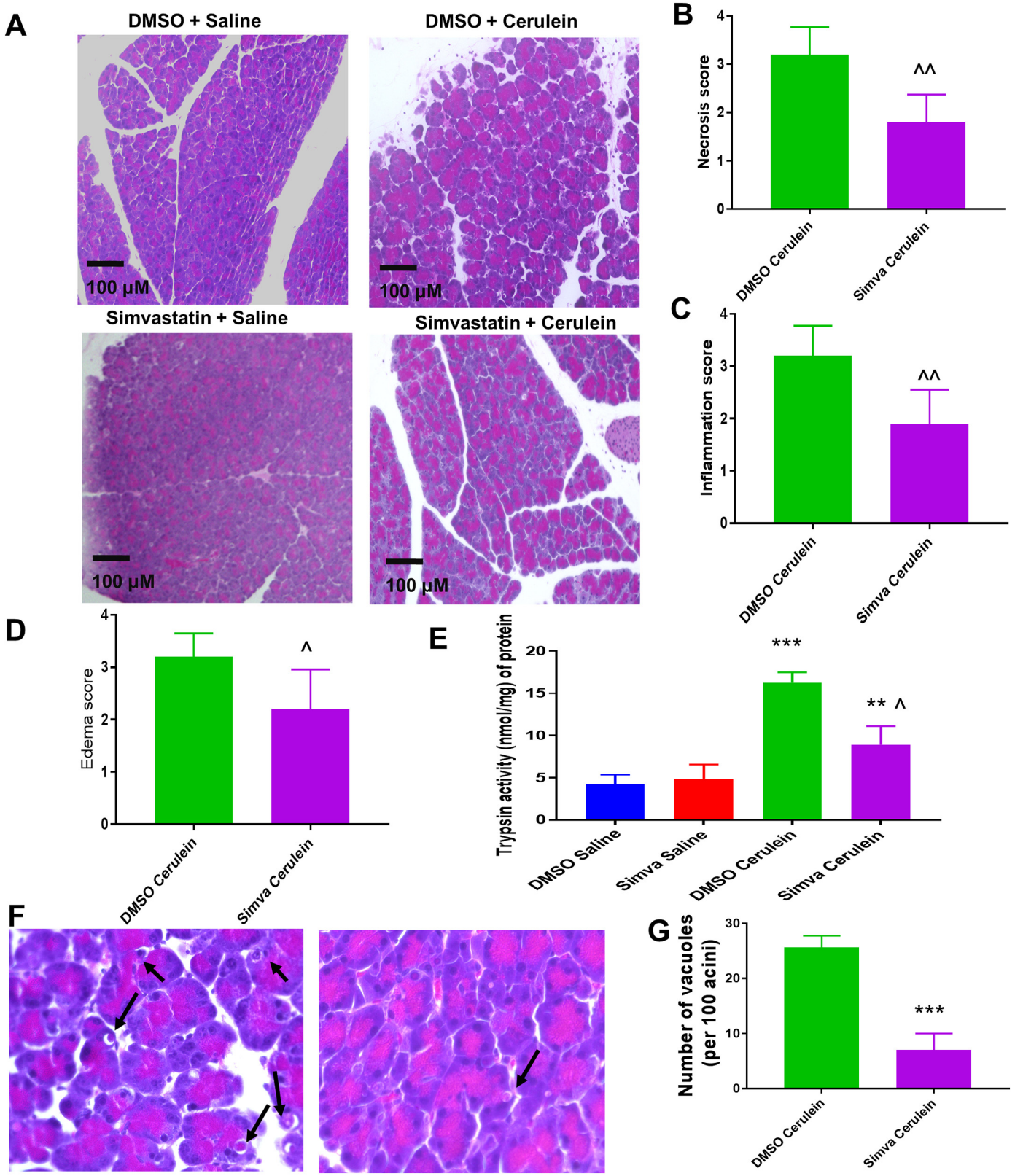

Fig. 1. Simvastatin reduces edema, cell death, and trypsin activation during acute pancreatitis. (A) Representative images of H&E staining of pancreatic tissue ($n = 5$). Bar graph indicates Necrosis score (B), Inflammation score (C) and Edema score (D) for each group on a scoring system of 1–4. Data shown are Mean ± SD. (E) Trypsin activity was measured by colorimetric assay. Histogram represents the trypsin activity (nmol/mg) for different groups. (F) Representative images of H&E staining of pancreatic tissue. (G) Bar graph represents the number of vacuoles per 100 acini. Values in graphs are represented as Mean ± SD, $^{**}p < 0.01$, $^{***}p < 0.001$ vs DMSO Saline; $\hat{}p < 0.05$, $\hat{}\hat{}p < 0.01$ vs DMSO Cerulein.

2.5. Subcellular fractionation for mitochondrial enrichment

Freshly isolated pancreatic tissue was homogenized via polytron using ice cold HES buffer containing 250 mM sucrose, 1 mM EDTA, and 10 mM 4-(2hydroxyethyl)-1-piperazine ethanesulfonic acid (HEPES) (pH 7.4) with protease inhibitor cocktail and phosphatase inhibitor (20 mM sodium fluoride). Samples were centrifuged at 1000 relative centrifugal force (rcf) for 10 min at 4 °C to remove large debris, unbroken cells and nucleus. A portion of resulting supernatant was saved as post-nuclear supernatant and 1% Triton X-100 was added (with protease inhibitor cocktail and phosphatase inhibitor cocktail). The remaining supernatant was transferred to a separate microfuge tube and further spun down at 1500 rcf for 5 min at 4 °C to remove zymogen granules. Resulting supernatant was further spun down at 7000 rcf for 10 min at 4 °C to obtain crude cytosolic (supernatant) and mitochondria-enriched heavy membrane fractions (pellet). Crude cytosol was transferred to a separate microfuge tube; the mitochondria-enriched heavy membrane fractions were washed with HES buffer and centrifuged at 7000 rcf for 5 min. The supernatant was discarded and pellet was resuspended in ice cold HES buffer containing 1% Triton X-100 (with protease inhibitor cocktail and phosphatase inhibitor cocktail). Post-nuclear supernatant and mitochondria-enriched heavy membrane fractions were stored in −80 °C freezer until use.

2.6. Trypsin activity assay

Trypsin activity in pancreatic samples was measured using Trypsin Activity Colorimetric Assay Kit (Sigma) according to the manufacturer's protocol.

2.7. Western blot analysis

Western blotting was performed according to the conditions and antibodies described in supplementary information.

2.8. Acini isolation, adenovirus infection and imaging

Acini were dispersed from pancreas surgically excised from 10 to 14 weeks old C57BL/6 (Charles river) mice as we previously described [29]. Adenovirus (mRFP-GFP-LC3 obtained from T. Yoshimori1) was constructed into an adenovirus by Vector Biolabs (Malvern, PA). Acini were treated with the adenovirus (1010 pfu/mL) and then further cultured for 14–16 h to express the LC3-GFP-RFP. The acini are then plated on glass coverslips for microscopy. The spinning disc confocal microscopy system is composed of an Olympus IX81 inverted fluorescence microscope (Center Valley, PA), a Yokogawa CSU X1 spinning disc confocal scan head (Yokogawa Electric Corporation, Tokyo, Japan), a diode-pumped solid state laser set (405 nm, 491 nm, 561 nm, 605 nm) (Spectral Applied Research, Concord, ON, Canada), a Hamamatsu C9100-13 EM-CCD (Hamamatsu Photonics, Shizuoka, Japan) and Volocity 3DM software (Perkin Elmer Corporation, Waltham, MA). Imaging of the acini was conducted at 37C (heated chamber), and the imaging data analyzed by Fiji, based on ImageJ 1.51 h (Wayne Rasband, National Institutes of Health, Bethesda, MD).

2.9. Electron microscopy

For electron microscopy, portions of fresh tissue were fixed in 3% glutaraldehyde, embedded in plastic, and cut into ultrathin sections. Sections were then stained with uranyl acetate and lead citrate and examined in a JEOL JEM-1010 or 100CX transmission electron microscope (JEOL Ltd., Tokyo, Japan). Several types of vacuoles were examined and counted performed independently by an individual who was blinded to the experimental groups.

2.10. mtDNA analysis

DNA extraction was performed from human and mouse plasma samples with a DNeasy® Blood&Tissue Kit (QIAGEN, Venlo, Netherlands) following the manufacturer's protocol. Before isolating the DNA, we added 0.5 ng (0.1 ng/μL) of a Green fluorescent protein (GFP)-plasmid to each sample, which further served as spiking control to normalize the mitochondrial DNA (mtDNA). Once the DNA was isolated, we performed a real-time polymerase chain reaction (PCR) for ND4 (mitochondrial gene) and GFP with a SYBR® Green real-time PCR kit (BIO-RAD, Hercules, CA, USA).

2.11. Network analysis and gene ontology

The Interaction maps of the proteins of interest (ULK1, LAMP1, PRKAA2(AMPK)) were extracted from a global human proteome interaction map dataset. Human proteome was collected from public databases containing non-redundant, loops exempt, experimentally validated undirected physical protein-protein binary interactions [30,31]. The protein interaction maps were visualized using Cytoscape and centrality measures of proteins, which provides relative importance of proteins within the network were calculated using Netanalyzer [32]. Gene ontological studies for identifying biological processes and pathways annotations for shared protein interactions among ULK-1 and AMPK protein were analyzed using ClueGO [33].

2.12. Statistical analysis

All values are presented as mean ± standard deviation. One-way ANOVA test was used to compare the groups. $P < 0.05$ was considered as statistically significant. All the statistical analysis was performed on GraphPad Prism v.7.

3. Results

3.1. Simvastatin pretreatment reduces inflammation and cell death during acute pancreatitis

A recent cohort analysis showed the reduced occurrence of pancreatitis risk with statin intake (especially simvastatin) in the Southern California Kaiser Permanente Health Care System [26]. To explore if simvastatin treatment could reduce the pancreatitis severity and to determine the mechanism of any beneficial effect, we employed an experimental pancreatitis model in mice using cerulein hyperstimulation. We pretreated the mice with simvastatin (20 mg/kg b.w.) for 24 h or DMSO (vehicle control), followed by 7 hourly intraperitoneal injections of cerulein (50 μg/kg each) to induce acute pancreatitis as illustrated. The animals were sacrificed 1 h after the last cerulein injection and tissue was collected for histology and other measurements. We found necrotic cell death, infiltration of inflammatory cells, and edema in the cerulein-treated pancreas, whereas simvastatin pretreatment attenuated this histopathology (Fig. 1A–D). Trypsin activation is one of the hallmarks of acute pancreatitis, whereby the cerulein treatment increases the trypsin activity in pancreatic tissue and promotes the pancreatitis response. We observed a significant reduction in trypsin activity with simvastatin pretreatment (Fig. 1E). Furthermore, we observed that simvastatin pretreatment reduced the vacuole accumulation (Fig. 1F–G) commonly seen in pancreatic acinar cells during acute pancreatitis.

3.2. Cerulein-induced acute pancreatitis stimulates mitophagy in mice

As we have previously shown that oxidative stress induces mitophagy as a cell survival defense mechanism [34], we next sought to determine if there is a mitophagy induction in our model of acute pancreatitis. Consistent with previous publications [11], we found a

significant increase in the levels of total (post-nuclear supernatant) p62 and lipidated LC3 after cerulein injections suggesting autophagy effects of cerulein (Fig. 2A–B). Next, we measured the mitophagy marker, parkin, and found that parkin abundance was significantly reduced during acute pancreatitis (Fig. 2A–B). Furthermore, we observed increased translocation of parkin to the mitochondria after cerulein exposure (Fig. 2C–D), which suggests the induction of mitophagy during pancreatitis. This is further confirmed using electron microscopy where

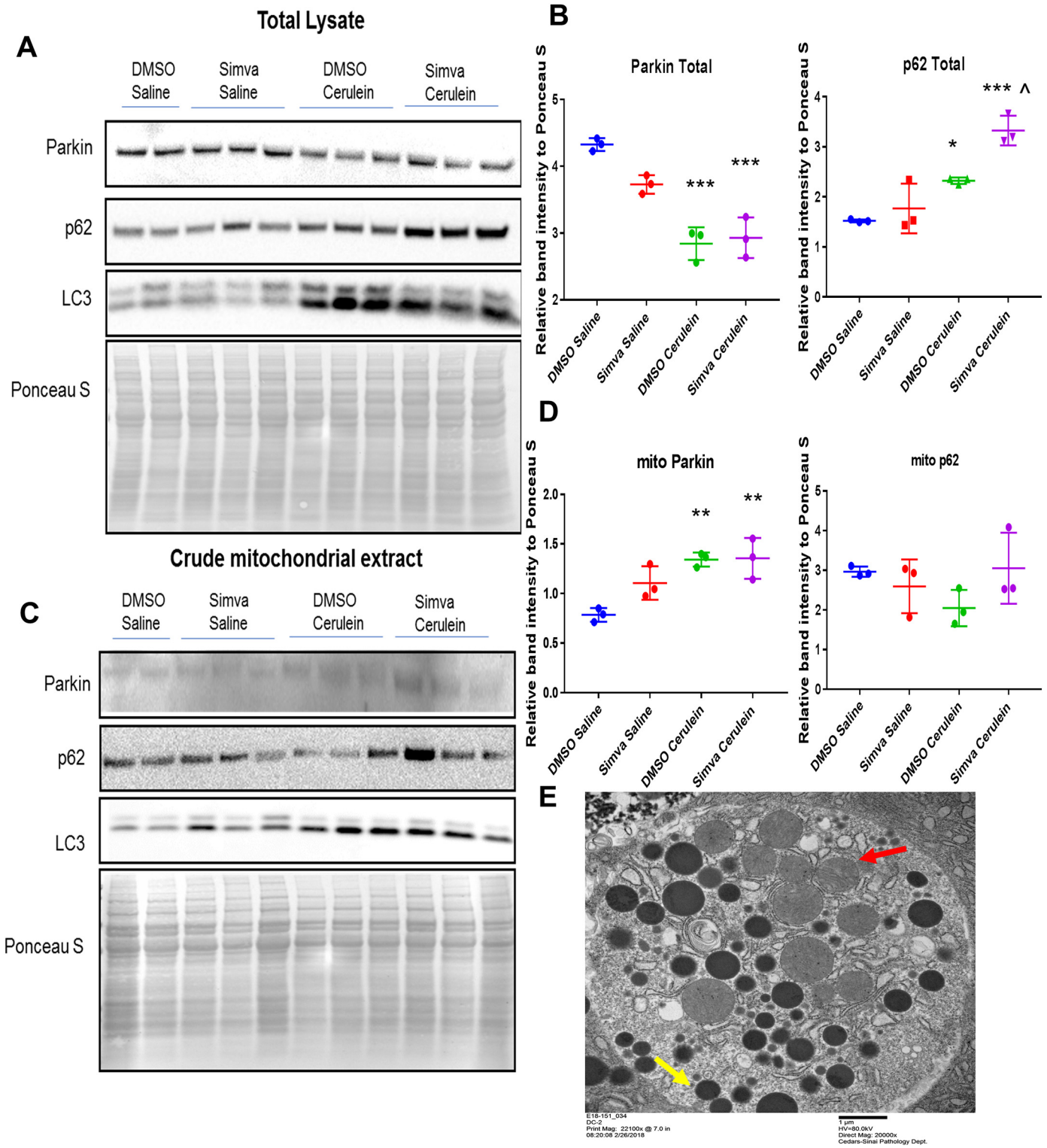

Fig. 2. Cerulein-induced pancreatitis triggers mitophagy. Mouse pancreatic tissue was collected and tissue lysates were fractionated for post-nuclear supernatant and crude mitochondrial fraction. (A) Western blot of post-nuclear supernatant for parkin, p62 and LC3. Ponceau S staining was used to normalize the protein expression. (B) Dot plots representing the expression of total parkin and total p62 normalized to Ponceau S stain. (C) Western blot showing expression of parkin, p62 and LC3 in crude mitochondrial fractions. (D) Dot plots representing the expression of mitochondrial parkin and p62 normalized to Ponceau S stain. Values in graphs are represented as Mean ± SD ($n = 3$), *$p < 0.05$, **$p < 0.01$, ***$p < 0.001$ vs DMSO Saline; ^$p < 0.05$ vs DMSO Cerulein. (E) Representative image of autophagy vacuole containing mitochondria (red arrow) along with other organelles including ER and zymogen Granules (yellow arrow).

mitochondria were present in autophagic vacuoles (Fig. 2E and Supplementary Fig. 2). Interestingly, simvastatin treatment (Simva-Cerulein) significantly increased p62 compared to DMSO-Cerulein (Fig. 2A–B). Also, there was no significant change in LC3 expression during pancreatitis with simvastatin pretreatment.

3.3. Cerulein impairs and simvastatin treatment preserves autophagosome-lysosome fusion

As previously shown, pancreatitis causes an accumulation of vacuoles, leading to cellular dysfunction [10]. Using electron microscopy,

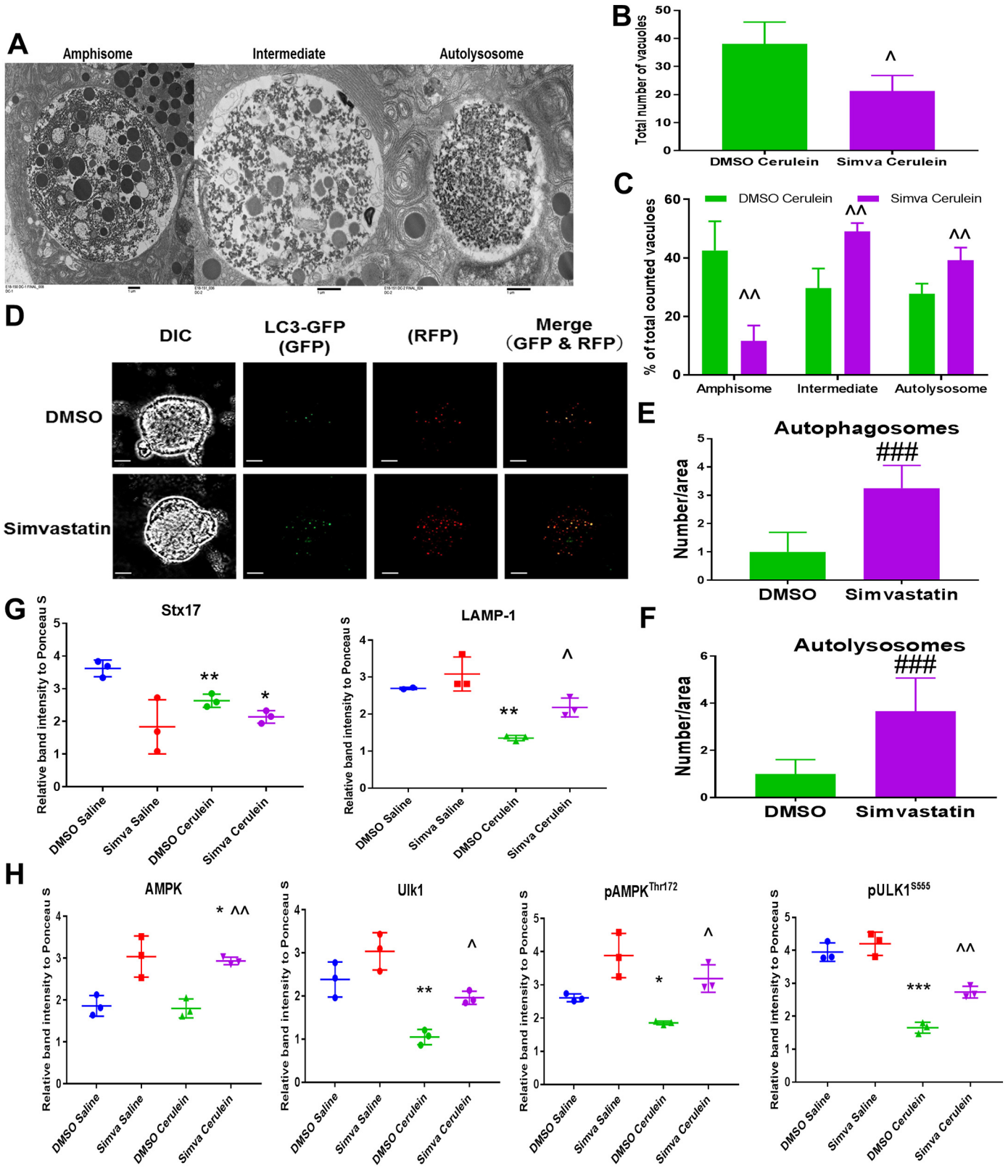

(caption on next page)

we found that the total number of vacuoles in the simvastatin pretreatment group was significantly reduced compared to DMSO control during acute pancreatitis (Fig. 3A). We counted the number of autophagosomes (recognizable cargo), intermediate vacuoles and autolysosomes (digested cargo) as a percent of the total number of vacuoles (Fig. 3B). Simvastatin pretreatment increased the number of intermediate vacuoles and autolysosomes, consistent with enhanced autophagic function with promotion of autophagosomes to functioning autolysosomes after cerulein exposure (Fig. 3C). To determine if simvastatin induced autophagy, we used the mRFP-GFP-LC3 reporter in isolated acini. Here, mRFP-GFP-LC3 fluoresces both red and green, represented as yellow in merged images, representing autophagosomes; when the autophagosome fuses with a lysosome to form an autolysosome, the lysosome's acidic pH quenches the GFP; thus, the mRFP-GFP-LC3 fluoresces red [35]. Under basal conditions (Fig. 3D–F), treatment of mouse pancreatic acini with 1 μM simvastatin increased the number of both autophagosomes and autolysosomes, indicating that simvastatin induced autophagic flux.

We next investigated the potential mechanisms underlying the preventing effects of simvastatin. Depletion of syntaxin 17 (Stx17), located on the outer membrane of the autophagosome, causes autophagosome accumulation [36]. Interestingly, although we found a decrease in the expression of Stx17 after cerulein injections, simvastatin didn't prevent Stx17 decrease during pancreatitis (Fig. 3G and Supplementary Fig. 3A), suggesting that cerulein effects on autophagy are in part due to decreased Stx17 but that simvastatin's protective effects are Stx17 independent. We next examined pancreatic levels of LAMP-1, ULK-1 and AMPK, which are essential for mitochondrial targeting to lysosomes [21] and functioning of autophagy [22,37]. We found that cerulein treatment significantly reduced LAMP-1 and ULK-1 protein expression, while AMPK levels didn't change (Fig. 3G–H and Supplementary Fig. 3A–B). As AMPK phosphorylates ULK-1 [21] to regulate the autophagosome-lysosome fusion process promoting normal autophagic progression, and the activity of both proteins is largely dependent on their phosphorylation states, we next determined the phosphorylation levels of $AMPK^{T172}$ and $ULK\text{-}1^{S555}$ and found that both $AMPK^{T172}$ and $ULK\text{-}1^{S555}$ were dephosphorylated after cerulein treatment (Fig. 3H and Supplementary Fig. 3B), suggesting the possibility that in experimental pancreatitis, the dephosphorylated state of these regulators could lead to cerulein-induced disorders in autophagy, specifically autophagosome-lysosome fusion. Simvastatin pretreatment upregulated LAMP-1, AMPK-1 and ULK-1 as well as the phosphorylated forms of AMPK and ULK-1 (Fig. 3G and Supplementary Fig. 3B), suggesting that simvastatin preserves autophagosome-lysosome fusion to promote autophagic flux.

3.4. mtDNA release during acute pancreatitis

Cells such as neutrophils with dysfunctional autophagosome-lysosome fusion are known to release mtDNA and associated protein transcription factor A, mitochondrial (TFAM) into the blood [38]. As pancreatitis showed a similar impairment of autophagic flux, we next tested if there was increased mtDNA release with pancreatitis and whether simvastatin could abrogate this effect. Using plasma obtained from healthy individuals and patients with acute pancreatitis, we determined mtDNA content by amplification of *ND4* normalized to a spiked-in control plasmid (*GFP*). Our findings revealed higher levels of mtDNA in plasma from acute pancreatitis patients compared to normal controls (Fig. 4A). We next determined if simvastatin could reduce mtDNA release into plasma in the cerulein-induced acute pancreatitis model in mice. We detected a tendential increase ($p = 0.23$) in mtDNA in plasma samples from cerulein-exposed mice, which was attenuated with simvastatin treatment (Fig. 4B). These findings support the importance of efficient autophagosome-lysosome fusion in preventing the release of inflammatory molecules such as mtDNA, which is a ligand for TLR9 [39] and the NLRP3 inflammasome [40].

3.5. Mitochondrial biogenesis is an early event in acute pancreatitis

Previous studies have shown that cellular stress signaling pathways can increase mitochondrial biogenesis to meet increased energy demand [41]. To determine if pancreatitis induces mitochondrial biogenesis, we determined the abundance of representative Oxidative phosphorylation (OXPHOS) subunits (CI-NDUFB8, CII-SDHB, CIII-UQCRC2, CIV-MTCO1, CV-ATP5A) and COXIV by western blot. We found that cerulein administration significantly increased the abundance of mitochondrial proteins (Fig. 5A–B and Supplementary Fig. 4) in both DMSO- and simvastatin-treated mice, although there was a trend of smaller increase of these proteins with simvastatin treatment. To understand the mechanism of mitochondrial biogenesis during pancreatitis, we performed a time-course study where mice were injected with 1, 3, or 7 cerulein injections (50 μg/kg per injection at hourly intervals) and sacrificed 1 h after last injection. We detected an increase in mitochondrial proteins as early as 1 h after the first cerulein injection (Fig. 5C–D), raising the possibility of a translationally-controlled process, possibly regulated through microRNAs.

3.6. Simvastatin increases stress resistant mitochondrial population

Previously, we reported that simvastatin induces mitophagy to provide cardioprotection during ischemia-reperfusion injury [28]. We next questioned if simvastatin induced mitochondrial quality control to prevent acinar cell injury. We assessed mitophagy in mouse pancreatic tissue obtained at various times after simvastatin administration, using mitophagy-related markers, parkin and mfn2, as well as autophagy-related markers, p62 and LC3. We observed a decrease in p62 at 3 h which returned to baseline (or slight increase) at 6 h, which was paralleled (with smaller changes) by Mfn2. Parkin and LC3 levels were lowest at 6 h and returned to baseline by 12 h (Fig. 6A). Mitochondrial protein abundance reached a nadir at 12 h, followed by partial recovery at 24 h (Fig. 6B). To determine if simvastatin depended on autophagic flux to induce clearance of dysfunctional mitochondria, we used chloroquine to prevent lysosomal acidification and fusion of autophagosomes with lysosomes. We then assessed the levels of p62 and OXPHOS proteins. Consistent with our earlier results (Fig. 6B), simvastatin triggered a decrease in OXPHOS proteins and p62, which was abolished by chloroquine administration (Fig. 6C–D). We hypothesized that simvastatin treatment would leave behind a population of mitochondria that were more stress-resistant. We performed mitochondrial swelling assays on mitochondria isolated from pancreas 24 h after treating the mice with DMSO or simvastatin. Mitochondria were resuspended in

Fig. 3. Simvastatin pretreatment improves autophagosome-lysosome fusion by enhanced autophagy signaling and preservation of LAMP-1 protein. (A) Pancreatic tissue was scored for different types of vacuoles by electron microscopy. Representative images show Amphisome, Intermediate vacuoles and autolysosomes in pancreatic sections. (B) Bar graph represents the total number of vacuoles during acute pancreatitis with DMSO (DMSO Cerulein) or simvastatin (Simva Cerulein) pretreatment ($n = 4$). Vacuoles were counted from at least 30 different fields for each group. (C) Several types of vacuoles (Amphisomes, Intermediate and Autolysosomes) were counted and expressed as percentage of total vacuoles. Values in graphs are represented as Mean ± SD. (D) Isolated mouse acini were transduced with Ad-LC3-GFP-RFP along with pretreatment with 1 μM simvastatin (dissolved in DMSO) or DMSO (control) for 16 h, and then fixed with 4% PFA. The slides were then observed under a spinning disc confocal microscope. Images shown are representative data. Bar graph represents the (E) total number of yellow (autophagosomes) and (F) red dots (autolysosomes) per area. Values in graphs are represented as Mean ± SD of 3 independent experiments, $^{###}p < 0.001$ vs DMSO. (G) Dot plots representing the expression of Stx17 and LAMP-1 (H) AMPK, ULK1, pAMPK (T172) and pULK1 (S555) normalized to Ponceau S stain. Values in graphs are represented as Mean ± SD ($n = 3$), $^{*}p < 0.05$, $^{**}p < 0.01$, $^{***}p < 0.001$ vs DMSO Saline; $^{\wedge}p < 0.05$, $^{\wedge\wedge}p < 0.01$ vs DMSO Cerulein.

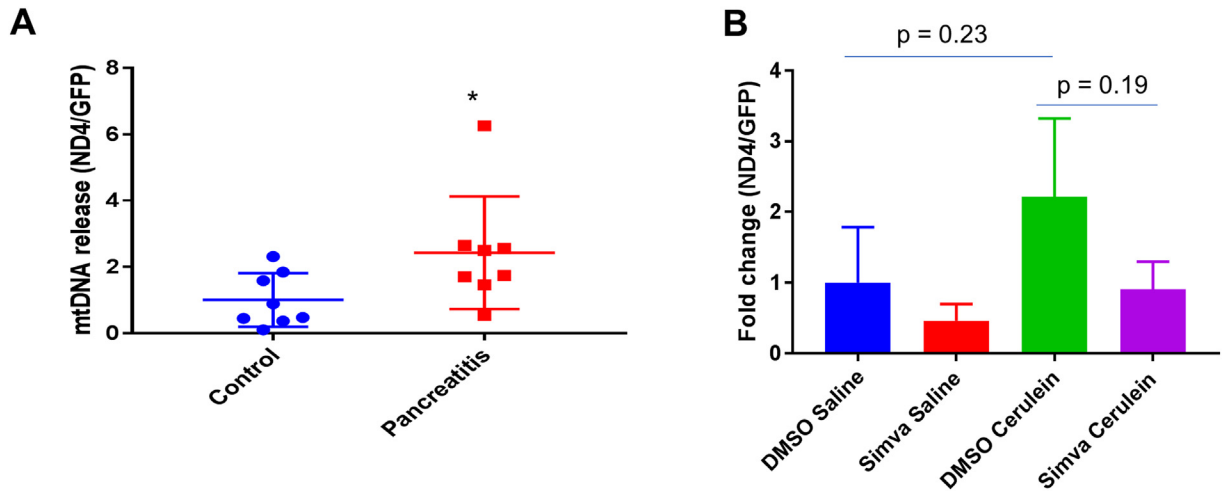

Fig. 4. Effects of pancreatitis and simvastatin treatment on mtDNA release. (A) Quantification of mtDNA release in blood assessed by qRT-PCR of mitochondrial gene *ND4* (fold change) present in plasma of normal control ($n = 8$) and acute pancreatitis patients (n = 8). GFP plasmid was spiked in before DNA extraction to normalize the samples. (B) Bar graph represents the quantification of *ND4* gene normalized to GFP, from plasma of mice treated with DMSO or simvastatin for 24 h followed by saline or cerulein (7 hourly) injections (n = 3). Values in graphs are represented as Mean ± SD, *p < 0.05 vs Control.

mitochondria swelling buffer and the decrease in absorbance was monitored after the addition of calcium (100 μM). Mitochondria from simvastatin-treated mice showed less swelling (decrease in absorbance) over the 20-minute observation (Fig. 6E), suggesting that simvastatin-induced mitochondria quality control resulted in a mitochondrial population that was more resistant to calcium overload.

3.7. Simvastatin protective effects are abolished with parkin genetic deletion

As previously shown by our group [28] in ischemia-reperfusion model of cardiac injury, simvastatin protection is parkin-dependent. We elucidated the role of parkin in pancreatic injury and whether parkin is required for simvastatin-induced protection. We used the same model as above and compared the effects of simvastatin in preventing pancreatic injury in parkin knockout (PKO) mice to wild type mice (wt-mice). At baseline, pancreatic tissue had normal histological appearance (Data not shown). However, simvastatin's protective effects against cerulein-induced pancreatitis were abolished with parkin deletion (Fig. 7A–D). Examination of p62 and AMPK revealed that both proteins were upregulated in PKO mice even in control saline groups, while simvastatin pretreatment further increased p62 and AMPK during pancreatitis (Fig. 7E–G). Also, decrease in COXIV expression with simvastatin pretreatment was abolished in PKO mice (Fig. 7E–F). We also noted increased accumulation of LC3 in PKO mice pretreated with simvastatin.

3.8. Network analysis for biological processes

As impaired flux is known to be involved in progression of pancreatitis to pancreatic cancer [42] and simvastatin helps resolve the process by activating AMPK and ULK-1, we next tried to determine the biological processes which can be affected by AMPK and ULK-1 dysregulation. We generated a protein-protein interaction network from whole human proteome showing 156 and 55 interacting proteins of AMPK and ULK-1 respectively (Fig. 8). Based on the network, biological processes involved were extracted using ClueGo-CluePedia. ULK1 and PRKAA2 and their shared interacting partners are enriched for pathway terms as well as biological processes. Network shows ULK-1 and AMPK (PRKAA1 and PRKAA2) linked with pathway terms showing their participation in biological processes especially mTOR signaling, p53 signaling, and energy homeostasis. Many of the enriched biological processes especially mTOR signaling, p53 signaling, and energy homeostasis are the key hallmarks of pancreatic cancer progression, underscoring the importance of activating AMPK and ULK-1 by simvastatin to mitigate pancreatitis.

4. Discussion

Accumulation of dysfunctional mitochondria owing to the blockage of autophagosome-lysosome fusion causes zymogen activation leading to necrotic cell death in pancreatitis. Clinical samples from acute pancreatitis also showed autophagic flux with accumulation of autophagic vacuoles [9]. We have reported for the first time the effects of simvastatin during experimental acute pancreatitis. Pancreatitis induces trypsinogen activation which is responsible for nearly 50% of pancreatic damage, but is not involved in inflammatory responses [43]. We found that simvastatin treatment reduces necrotic cell death associated with reduced trypsinogen activation. Attenuation of pancreatitis is largely dependent on the resolution of inflammation [44], and simvastatin reduced the infiltration of inflammatory cells.

Mitophagy has been studied in detail as a defense mechanism in other organs, with multiple findings that mitophagy-inducing drugs can reduce cellular injury [45]. Mitophagy or autophagy impairment can lead to decline in cell survival and accelerates aging [46]. Studies are lacking on the impact of mitophagy in pancreatitis. Our findings suggest the role of parkin in inducing mitophagy whereby it translocates to mitochondria in pancreatitis. However, further studies need to be done to study mitophagy in detail using reporter mice such as mito-QC mice and parkin-independent mechanisms of mitophagy. Also, pancreatitis impairs autophagic flux [13] by downregulating expression of LAMPs necessary for autophagosome-lysosome fusion. Due to altered Cathepsin B maturation, LAMPs get degraded, contributing to chronic pancreatitis [20]. Our findings revealed downregulation of LAMP-1 in pancreatitis, which was prevented by simvastatin. In the absence of efficient autophagic flux, there is accumulation of dysfunctional mitochondria which are sensitive to calcium overload [47]. We also found AMPK and ULK-1 to be altered during pancreatitis. These factors play a key role in mitophagy and autophagosome-lysosome fusion [23]. We found that simvastatin triggers phosphorylation of AMPK on threonine172 (activating site). Active AMPK phosphorylates ULK-1 on serine555 to activate it [22]. This complex is known to be an important mediator in targeting mitochondria to lysosomes, as well as to activate autophagic flux [21]. We found that during acute pancreatitis there was downregulation of both ULK-1 and its phosphorylated form. However, AMPK and ULK1 have important roles in PI3P production and autophagosome formation in various cell types. We found that autophagy

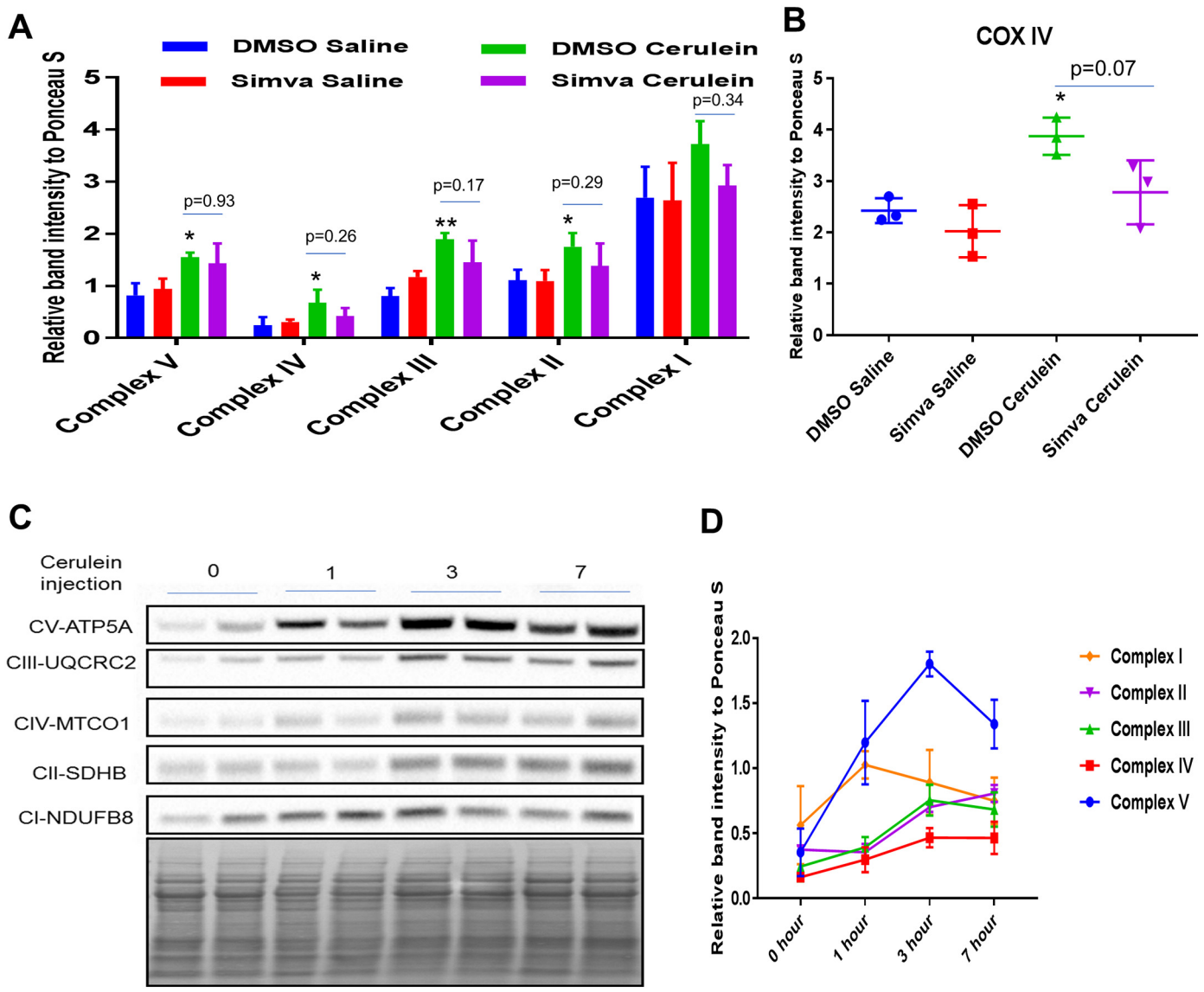

Fig. 5. Upregulation of mitochondrial proteins occurs rapidly after cerulein exposure. (A) Graphs representing the Ponceau S stained normalized protein expression of ATP5A (Complex V), MTCO1 (Complex IV), UQCRC2 (Complex III), SDHB (Complex II), NDUFB8 (Complex I) and (B) COX IV. (C) Different number of (1, 3 or 7) Cerulein injections (50 μg/kg, i.p. per injection, each at 1-hour interval) were administered and mice were sacrificed 1 h after indicated cerulein injections to collect pancreatic tissue. Control mice received no injection (0 h). Western blot showing expression of ATP5A (Complex V), MTCO1 (Complex IV), UQCRC2 (Complex III), SDHB (Complex II), NDUFB8 (Complex I) subunits of mitochondrial electron transport machinery. (D) Line graph represents the Ponceau S staining normalized expression of these proteins at different times after cerulein injections. Values in graphs are represented as Mean ± SD (n = 3), *p < 0.05, **p < 0.01, ***p < 0.001 vs DMSO Saline.

was activated despite the decreased abundance of active AMPK and ULK1. The role of ULK1 in autophagy initiation during pancreatitis is yet unknown and there may be additional proteins involved in autophagy initiation (such as non-canonical autophagy, which is independent of PI3K and involves Rubicon [48]). ULK1 downregulation in this model implicates a role for ULK1 in the fusion process in cerulein-induced acute pancreatitis model. However, to examine the possibility and to dissect the molecular function of ULK1 in pancreatitis, more detailed studies are needed. Simvastatin treatment helped to restore the expression of ULK-1 as well as its phosphorylation, restoring autophagic flux. Shugrue et al. (2012) showed that early AMPK activation can prevent cerulein-induced zymogen activation [49]. Our results are based on Triton X-100-soluble AMPK levels, and we did not assess Triton X-100-insoluble AMPK. It will be interesting to determine whether simvastatin alters the distribution of AMPK in acinar cells. Additionally, syntaxin 17 (Stx17, autophagosomal SNARE) binds to other lysosomal SNARE proteins to enable completion of the fusion process [50]. We observed that Stx17 expression was decreased by simvastatin treatment as well as by pancreatitis, suggesting that the beneficial effect of simvastatin was Stx17 independent. Further studies need to be done to elucidate the role of SNARE proteins in pancreatitis [51].

Coordination of mitophagy and mitochondrial biogenesis is required for mitochondrial homeostasis [52]. Pancreatitis causes ATP depletion due to mitochondrial dysfunction, and damaged mitochondria also generate reactive oxygen species (ROS), contributing to tissue damage [53]. High energy demands during cellular insults like pancreatitis may stimulate mitochondrial biogenesis for energy homeostasis. Our results reveal an increase in mitochondrial biogenesis as early as 1 h after cerulein injection, suggesting that the process may be translationally controlled, and may implicate regulation by microRNAs. Increased ROS production can oxidize mtDNA and lead to release of mtDNA by the cells into the blood; release of mtDNA has been

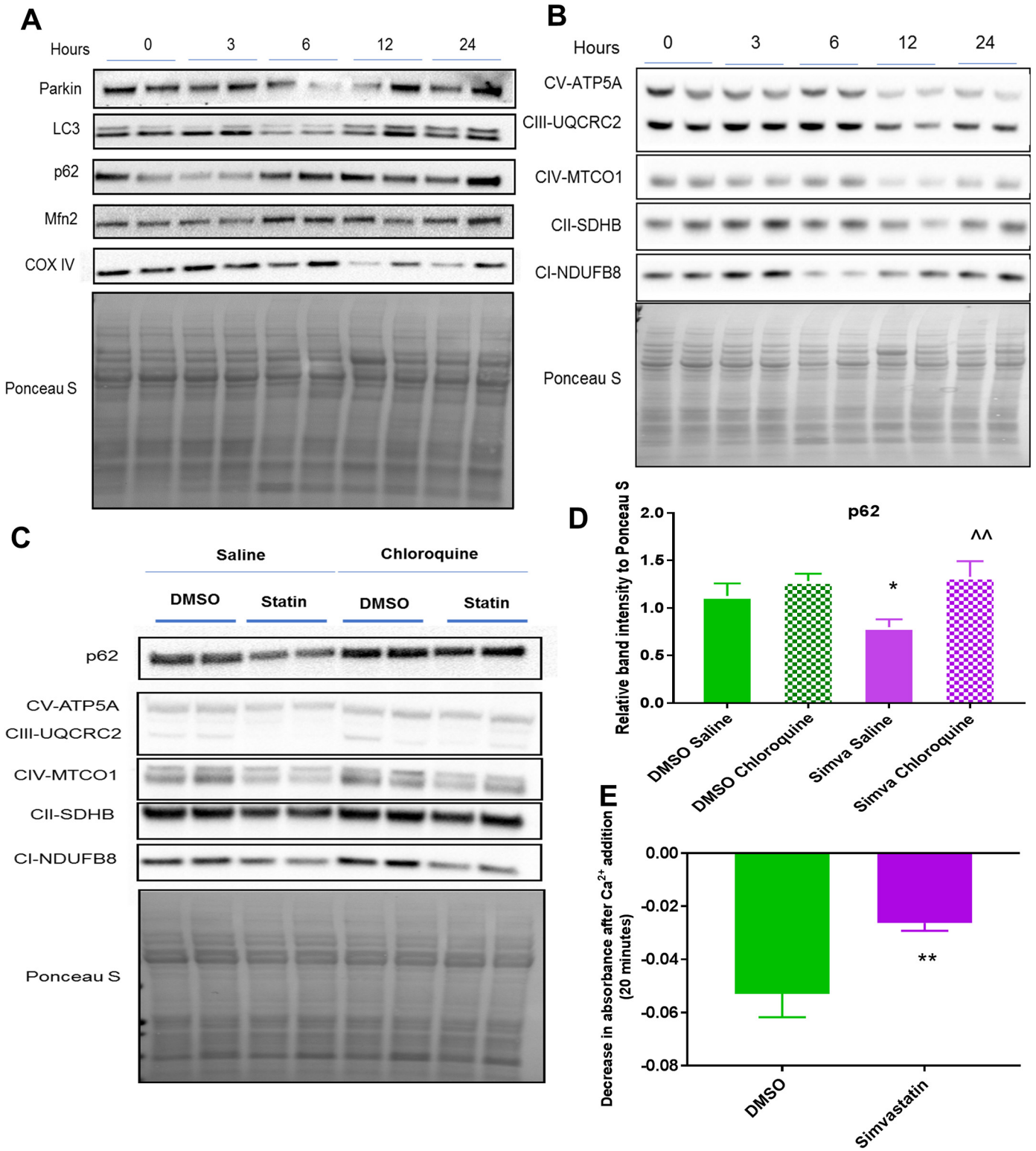

Fig. 6. Simvastatin induces mitophagy for mitochondrial quality control. Mice were treated with simvastatin and sacrificed 3, 6, 12, 24 h later. (A) Western blot for pancreatic tissue lysate showing the expression of Parkin and Mfn2, p62 and LC3. COX IV is used to indicate mitochondrial content in the lysate. Ponceau S staining was used as loading control. (B) Western blot for different mitochondrial subunits of OXPHOS complexes (ATP5A, UQCRC2, MTCO1, SDHB and NDUFB8) and used to infer mitochondrial content present in the lysate at the indicated time points. (C) Mice were pretreated with DMSO or simvastatin (20 mg/kg, i.p.) for 6 h followed by saline or chloroquine (40 mg/kg, i.p.) for 4 h and pancreatic tissue was processed to obtain post-nuclear supernatants. Representative western blot showing expression of p62, ATP5A, UQCRC2, MTCO1, SDHB and NDUFB8. (D) Bar graph represents the expression of p62, normalized to Ponceau S stain. Values in graphs are represented as Mean ± SD (n = 3), *p < 0.05 vs DMSO Saline; ^^p < 0.01 vs Simva Saline. (E) Mitochondrial swelling was used as an indicator of mitochondrial quality in pancreatic tissue from mice treated with DMSO or simvastatin (20 mg/kg) for 24 h. Bar graph represents the decrease in absorbance (540 nm) after incubating the isolated mitochondria with 100 μM Ca2+ for 20 min. Values in graphs are represented as Mean ± SD (n = 3), *p < 0.05, **p < 0.01 vs DMSO control.

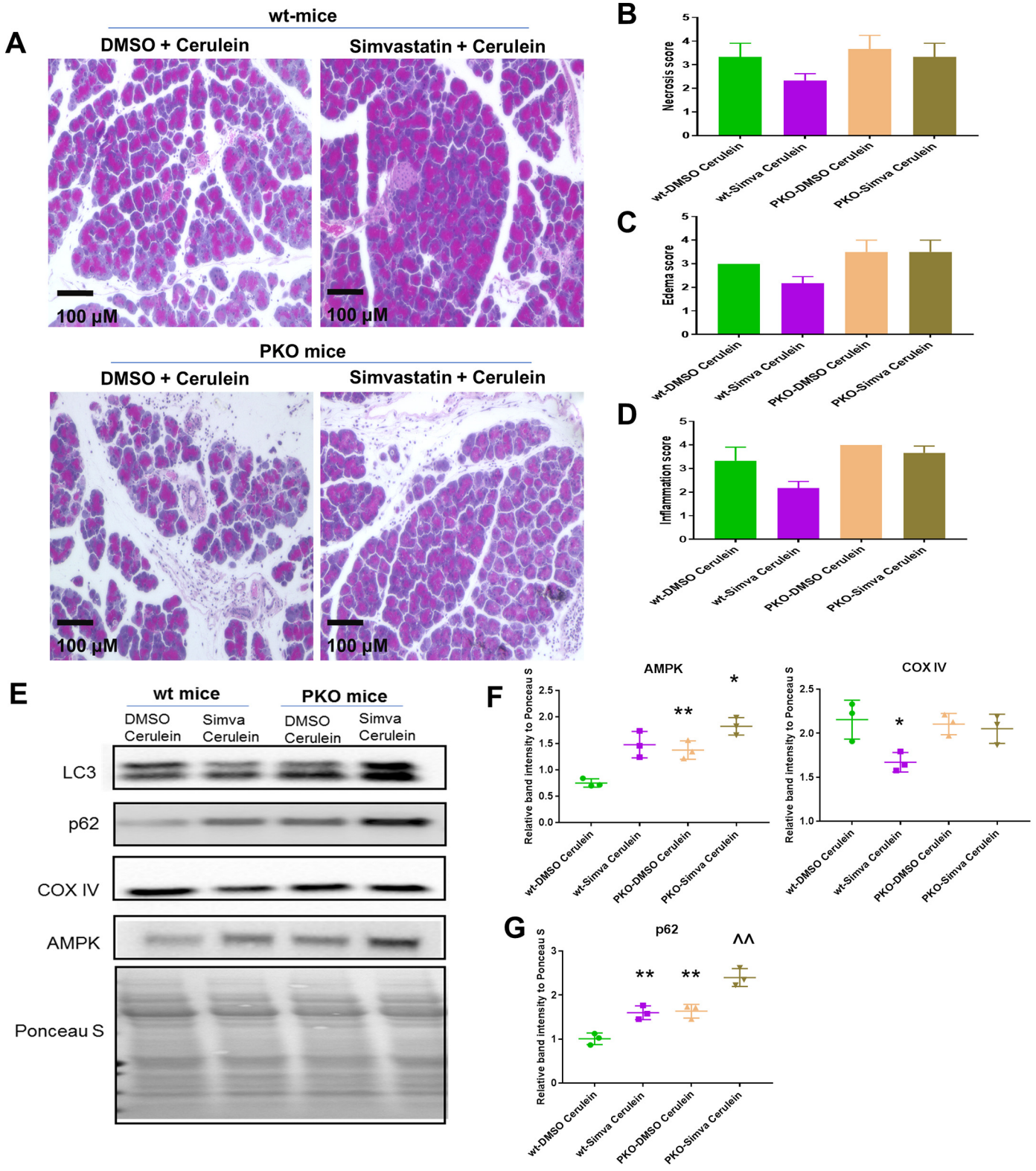

Fig. 7. Simvastatin-mediated protection is dependent on Parkin. Acute pancreatitis was induced in wild type (wt-mice) and Parkin knockout mice (PKO mice) with 7 hourly injections of cerulein. DMSO or simvastatin (20 mg/kg) was given 24 h before inducing acute pancreatitis. (A) Representative images of H&E stained pancreatic tissue from different groups. Bar graph indicates Necrosis score (B), Inflammation score (C) and Edema score (D) for each group on a scoring system of 1–4. Data shown are Mean ± SD. (E) Western blot showing the expression of LC3, p62, COX IV and AMPK. Dot plots representing the expression of (F) AMPK and COX IV, and (G) p62, all normalized to Ponceau S stain. Values in graphs are represented as Mean ± SD (n = 3), *p < 0.05, **p < 0.01 vs wt-DMSO Cerulein; ^^p < 0.01 vs PKO-DMSO Cerulein.

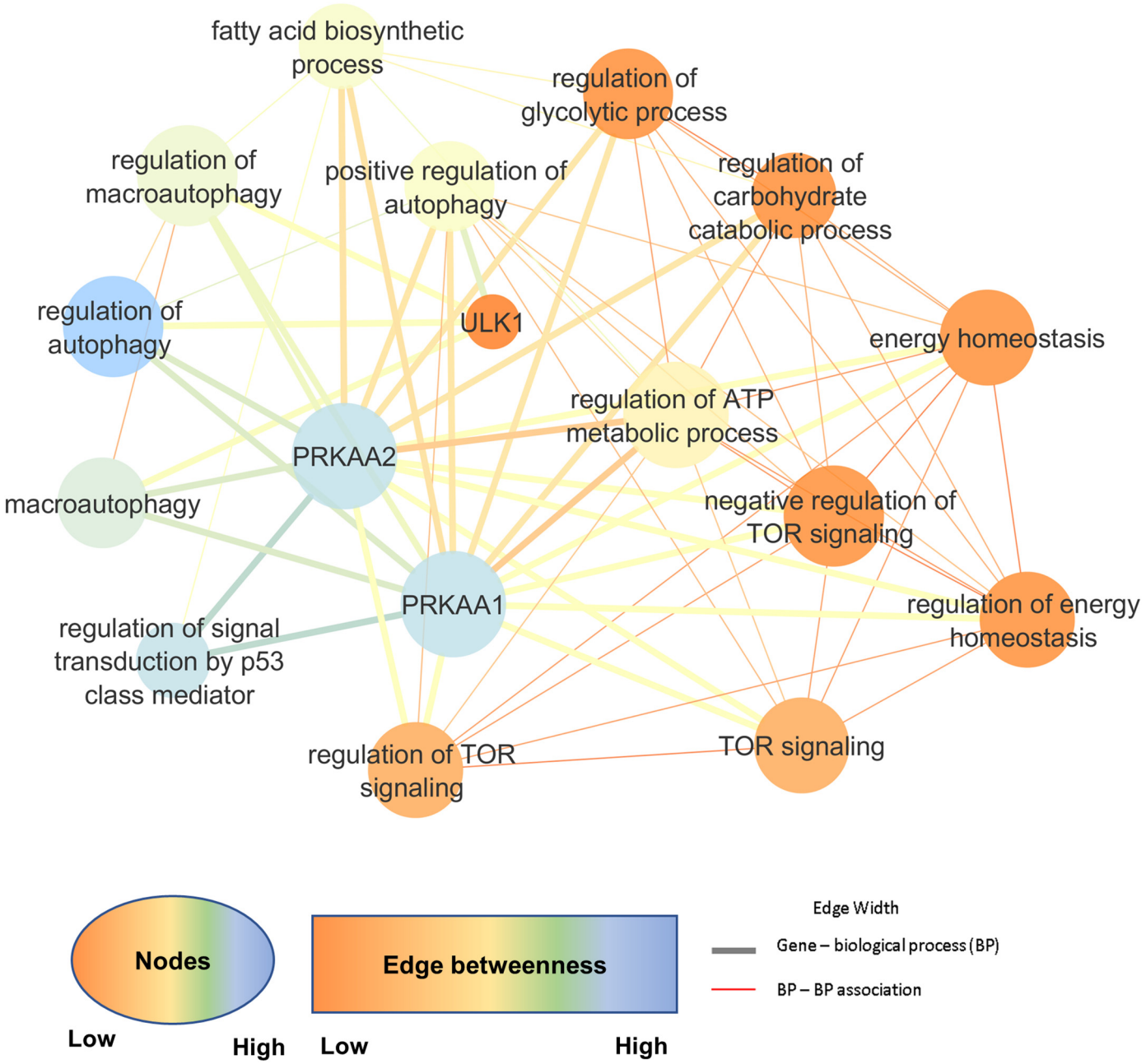

Fig. 8. BINGO/ClueGo Network analysis for protein-protein interaction of AMPK (*PRKAA2*) and ULK1 to identify different biological processes generated using Cytoscape. Edge betweenness centrality is the indicator of essentiality of that edge in the network. Degree is the number of connections related to the node in the network. Thick lines indicate the Gene to biological process (BP) association and thin lines indicate BP to BP association. Color of the node represents the importance of the node in the network.

implicated in many disease processes [54]. Also, impaired autophagic flux can enhance the release of mtDNA into the blood [38]. Mitophagy deficiency can lead to enhanced mtDNA release and can lead to inflammation. Recently, Bueno et al. (2019) suggested the role of mitophagy in the attenuation of mtDNA release [55]. Our findings confirm the presence of increased mtDNA in plasma of mice and humans with pancreatitis, suggesting the impairment of mitophagy and autophagy flux. These mtDNA molecules can further act as ligands for innate immunity [56] via NLRP3 inflammasome activation and TLR9 signaling. Simvastatin may attenuate mtDNA release and thereby reduce inflammatory cell infiltration.

Parkin is an important mediator of mitophagy; it translocates from cytosol to mitochondria where it poly-ubiquitinates multiple proteins on the mitochondrial outer membrane. The process triggers recruitment of adapter proteins such as p62, leading to engulfment of mitochondria by LC3-decorated autophagosomes [57]. Previous findings from our lab suggested the importance of parkin in ischemic injury in heart [58] and the requirement of parkin for simvastatin-induced mitophagy in cardiac cells [28]. Here, we showed that simvastatin protective effects are abolished with parkin deletion.

Recent epidemiologic reports from our group showed that recurrence of pancreatic cancer after surgery was reduced in patients taking simvastatin [27]. Patients with pancreatitis have been associated with higher risk of developing pancreatic cancer. Autophagosome accumulation during pancreatitis can promote pancreatic cancer [56]. To determine the pathways which may be involved in the promotion of pancreatic cancer, our protein network analysis focused on two key factors altered by simvastatin—AMPK and ULK1—showed that AMPK

and ULK-1 affect many biological processes including p53 signaling, mTOR signaling, and energy homeostasis that can lead to promotion of cancer. However, further studies are needed to delineate the importance of simvastatin usage in reducing the promotion and recurrence of pancreatic cancer. Also, since there is a lack of therapeutics in treating pancreatitis, a clinical trial to determine the efficacy of simvastatin is appropriate give that it has been shown to be safe in patients.

5. Conclusion

To conclude, our findings implicate impaired autophagic flux in acute pancreatitis which can be corrected with simvastatin treatment. Thus, the findings support the importance of simvastatin as a therapeutic intervention for pancreatitis.

Supplementary data to this article can be found online at https://doi.org/10.1016/j.bbadis.2019.08.006.

Funding

This study was funded by NIH R01 HL132075 (to RAG), DoD W81XWH-17-1-0138 (to SJP), NIAAA P50 AA11999-subaward 98578050 (to HP), Canadian Institutes of Health Research PJT-159542 (HYG) and the Dorothy and E. Phillip Lyon endowed chair in Molecular Cardiology (to RAG). This study was also supported by NIH P50 AA11999 (to SJP), NIH P01 DK098108 (to SJP), NIH U01 DK108314 (to SJP) and NIH/DCP, NCI NWU2014 (to SJP).

Transparency document

The Transparency document associated with this article can be found, in online version.

Declaration of competing interest

None.

Acknowledgements

We would like to acknowledge the Cedars-Sinai Biobank and Translational research core for histology services.

References

[1] F.S. Gorelick, E. Thrower, The acinar cell and early pancreatitis responses, Clin. Gastroenterol. Hepatol. 7 (2009) S10–S14.
[2] S.J. Pandol, A.K. Saluja, C.W. Imrie, P.A. Banks, Acute pancreatitis: bench to the bedside, Gastroenterology 132 (2007) 1127–1151.
[3] R. Mukherjee, O.A. Mareninova, I.V. Odinokova, W. Huang, J. Murphy, M. Chvanov, M.A. Javed, L. Wen, D.M. Booth, M.C. Cane, M. Awais, B. Gavillet, R.M. Pruss, S. Schaller, J.D. Molkentin, A.V. Tepikin, O.H. Petersen, S.J. Pandol, I. Gukovsky, D.N. Criddle, A.S. Gukovskaya, R. Sutton, N.P.B.R. Unit, Mechanism of mitochondrial permeability transition pore induction and damage in the pancreas: inhibition prevents acute pancreatitis by protecting production of ATP, Gut 65 (2016) 1333–1346.
[4] A.S. Gukovskaya, S.J. Pandol, I. Gukovsky, New insights into the pathways initiating and driving pancreatitis, Curr. Opin. Gastroenterol. 32 (5) (2016) 429–435 Sep.
[5] A. Venkatraman, A. Landar, A.J. Davis, E. Ulasova, G. Page, M.P. Murphy, V. Darley-Usmar, S.M. Bailey, Oxidative modification of hepatic mitochondria protein thiols: effect of chronic alcohol consumption, Am. J. Physiol. Gastrointest. Liver Physiol. 286 (2004) G521–G527.
[6] R.A. Ehlers, A. Hernandez, L.S. Bloemendal, R.T. Ethridge, B. Farrow, B.M. Evers, Mitochondrial DNA damage and altered membrane potential (delta psi) in pancreatic acinar cells induced by reactive oxygen species, Surgery 126 (1999) 148–155.
[7] S.W. Ryter, S.M. Cloonan, A.M. Choi, Autophagy: a critical regulator of cellular metabolism and homeostasis, Mol. Cells 36 (2013) 7–16.
[8] D. Hashimoto, M. Ohmuraya, M. Hirota, A. Yamamoto, K. Suyama, S. Ida, Y. Okumura, E. Takahashi, H. Kido, K. Araki, H. Baba, N. Mizushima, K. Yamamura, Involvement of autophagy in trypsinogen activation within the pancreatic acinar cells, J. Cell Biol. 181 (2008) 1065–1072.
[9] K.N. Diakopoulos, M. Lesina, S. Wormann, L. Song, M. Aichler, L. Schild, A. Artati, W. Romisch-Margl, T. Wartmann, R. Fischer, Y. Kabiri, H. Zischka, W. Halangk, I.E. Demir, C. Pilsak, A. Walch, C.S. Mantzoros, J.M. Steiner, M. Erkan, R.M. Schmid, H. Witt, J. Adamski, H. Algul, Impaired autophagy induces chronic atrophic pancreatitis in mice via sex- and nutrition-dependent processes, Gastroenterology 148 (2015) 626–638 (e617).
[10] O.A. Mareninova, K. Hermann, S.W. French, M.S. O'Konski, S.J. Pandol, P. Webster, A.H. Erickson, N. Katunuma, F.S. Gorelick, I. Gukovsky, A.S. Gukovskaya, Impaired autophagic flux mediates acinar cell vacuole formation and trypsinogen activation in rodent models of acute pancreatitis, J. Clin. Invest. 119 (2009) 3340–3355.
[11] A.S. Gukovskaya, I. Gukovsky, Autophagy and pancreatitis, Am. J. Physiol. Gastrointest. Liver Physiol. 303 (2012) G993–G1003.
[12] N. Mizushima, A. Yamamoto, M. Matsui, T. Yoshimori, Y. Ohsumi, In vivo analysis of autophagy in response to nutrient starvation using transgenic mice expressing a fluorescent autophagosome marker, Mol. Biol. Cell 15 (2004) 1101–1111.
[13] I. Gukovsky, S.J. Pandol, A.S. Gukovskaya, Organellar dysfunction in the pathogenesis of pancreatitis, Antioxid. Redox Signal. 15 (2011) 2699–2710.
[14] B.G. Hill, G.A. Benavides, J.R. Lancaster Jr., S. Ballinger, L. Dell'Italia, Z. Jianhua, V.M. Darley-Usmar, Integration of cellular bioenergetics with mitochondrial quality control and autophagy, Biol. Chem. 393 (2012) 1485–1512.
[15] H.M. Ni, J.A. Williams, W.X. Ding, Mitochondrial dynamics and mitochondrial quality control, Redox Biol. 4 (2015) 6–13.
[16] C. Vives-Bauza, C. Zhou, Y. Huang, M. Cui, R.L. de Vries, J. Kim, J. May, M.A. Tocilescu, W. Liu, H.S. Ko, J. Magrane, D.J. Moore, V.L. Dawson, R. Grailhe, T.M. Dawson, C. Li, K. Tieu, S. Przedborski, PINK1-dependent recruitment of Parkin to mitochondria in mitophagy, Proc. Natl. Acad. Sci. U. S. A. 107 (2010) 378–383.
[17] G. Ashrafi, T.L. Schwarz, The pathways of mitophagy for quality control and clearance of mitochondria, Cell Death Differ. 20 (2013) 31–42.
[18] N. Zaarur, A.B. Meriin, E. Bejarano, X. Xu, V.L. Gabai, A.M. Cuervo, M.Y. Sherman, Proteasome failure promotes positioning of lysosomes around the aggresome via local block of microtubule-dependent transport, Mol. Cell. Biol. 34 (2014) 1336–1348.
[19] V. Hubert, A. Peschel, B. Langer, M. Groger, A. Rees, R. Kain, LAMP-2 is required for incorporating syntaxin-17 into autophagosomes and for their fusion with lysosomes, Biol Open 5 (2016) 1516–1529.
[20] O.A. Mareninova, M. Sendler, S.R. Malla, I. Yakubov, S.W. French, E. Tokhtaeva, O. Vagin, V. Oorschot, R. Lullmann-Rauch, J. Blanz, D. Dawson, J. Klumperman, M.M. Lerch, J. Mayerle, I. Gukovsky, A.S. Gukovskaya, Lysosome associated membrane proteins maintain pancreatic acinar cell homeostasis: LAMP-2 deficient mice develop pancreatitis, Cell. Mol. Gastroenterol. Hepatol. 1 (2015) 678–694.
[21] R.C. Laker, J.C. Drake, R.J. Wilson, V.A. Lira, B.M. Lewellen, K.A. Ryall, C.C. Fisher, M. Zhang, J.J. Saucerman, L.J. Goodyear, M. Kundu, Z. Yan, Ampk phosphorylation of Ulk1 is required for targeting of mitochondria to lysosomes in exercise-induced mitophagy, Nat. Commun. 8 (2017) 548.
[22] M. Zhao, D.J. Klionsky, AMPK-dependent phosphorylation of ULK1 induces autophagy, Cell Metab. 13 (2011) 119–120.
[23] W. Tian, W. Li, Y. Chen, Z. Yan, X. Huang, H. Zhuang, W. Zhong, Y. Chen, W. Wu, C. Lin, H. Chen, X. Hou, L. Zhang, S. Sui, B. Zhao, Z. Hu, L. Li, D. Feng, Phosphorylation of ULK1 by AMPK regulates translocation of ULK1 to mitochondria and mitophagy, FEBS Lett. 589 (2015) 1847–1854.
[24] A.M. Andres, A. Stotland, B.B. Queliconi, R.A. Gottlieb, A time to reap, a time to sow: mitophagy and biogenesis in cardiac pathophysiology, J. Mol. Cell. Cardiol. 78 (2015) 62–72.
[25] A.M. Andres, K.C. Tucker, A. Thomas, D.J. Taylor, D. Sengstock, S.M. Jahania, R. Dabir, S. Pourpirali, J.A. Brown, D.G. Westbrook, S.W. Ballinger, R.M. Mentzer Jr., R.A. Gottlieb, Mitophagy and mitochondrial biogenesis in atrial tissue of patients undergoing heart surgery with cardiopulmonary bypass, JCI Insight 2 (2017) e89303.
[26] B.U. Wu, S.J. Pandol, I.L. Liu, Simvastatin is associated with reduced risk of acute pancreatitis: findings from a regional integrated healthcare system, Gut 64 (2015) 133–138.
[27] B.U. Wu, J. Chang, C.Y. Jeon, S.J. Pandol, B. Huang, E.W. Ngor, A.L. Difronzo, R.M. Cooper, Impact of statin use on survival in patients undergoing resection for early-stage pancreatic cancer, Am. J. Gastroenterol. 110 (2015) 1233–1239.
[28] A.M. Andres, G. Hernandez, P. Lee, C. Huang, E.P. Ratliff, J. Sin, C.A. Thornton, M.V. Damasco, R.A. Gottlieb, Mitophagy is required for acute cardioprotection by simvastatin, Antioxid. Redox Signal. 21 (2014) 1960–1973.
[29] S. Dolai, T. Liang, A.I. Orabi, D. Holmyard, L. Xie, D. Greitzer-Antes, Y. Kang, H. Xie, T.A. Javed, P.P. Lam, D.C. Rubin, P. Thorn, H.Y. Gaisano, Pancreatitis-induced depletion of Syntaxin 2 promotes autophagy and increases basolateral exocytosis, Gastroenterology 154 (2018) 1805–1821 (e1805).
[30] G. Scardoni, M. Petterlini, C. Laudanna, Analyzing biological network parameters with CentiScaPe, Bioinformatics 25 (2009) 2857–2859.
[31] D. Pratt, J. Chen, D. Welker, R. Rivas, R. Pillich, V. Rynkov, K. Ono, C. Miello, L. Hicks, S. Szalma, A. Stojmirovic, R. Dobrin, M. Braxenthaler, J. Kuentzer, B. Demchak, T. Ideker, NDEx, the network data exchange, Cell Syst. 1 (2015) 302–305.
[32] Y. Assenov, F. Ramirez, S.E. Schelhorn, T. Lengauer, M. Albrecht, Computing topological parameters of biological networks, Bioinformatics 24 (2008) 282–284.
[33] G. Bindea, B. Mlecnik, H. Hackl, P. Charoentong, M. Tosolini, A. Kirilovsky, W.H. Fridman, F. Pages, Z. Trajanoski, J. Galon, ClueGO: a Cytoscape plug-in to decipher functionally grouped gene ontology and pathway annotation networks, Bioinformatics 25 (2009) 1091–1093.
[34] A. Hamacher-Brady, N.R. Brady, R.A. Gottlieb, Enhancing macroautophagy protects against ischemia/reperfusion injury in cardiac myocytes, J. Biol. Chem. 281 (2006) 29776–29787.
[35] S. Kimura, T. Noda, T. Yoshimori, Dissection of the autophagosome maturation

process by a novel reporter protein, tandem fluorescent-tagged LC3, Autophagy 3 (2007) 452–460.
[36] E. Itakura, N. Mizushima, Syntaxin 17: the autophagosomal SNARE, Autophagy 9 (2013) 917–919.
[37] E.L. Eskelinen, Roles of LAMP-1 and LAMP-2 in lysosome biogenesis and autophagy, Mol. Asp. Med. 27 (2006) 495–502.
[38] S. Caielli, S. Athale, B. Domic, E. Murat, M. Chandra, R. Banchereau, J. Baisch, K. Phelps, S. Clayton, M. Gong, T. Wright, M. Punaro, K. Palucka, C. Guiducci, J. Banchereau, V. Pascual, Oxidized mitochondrial nucleoids released by neutrophils drive type I interferon production in human lupus, J. Exp. Med. 213 (2016) 697–713.
[39] T. Oka, S. Hikoso, O. Yamaguchi, M. Taneike, T. Takeda, T. Tamai, J. Oyabu, T. Murakawa, H. Nakayama, K. Nishida, S. Akira, A. Yamamoto, I. Komuro, K. Otsu, Mitochondrial DNA that escapes from autophagy causes inflammation and heart failure, Nature 485 (2012) 251–255.
[40] K. Shimada, T.R. Crother, J. Karlin, J. Dagvadorj, N. Chiba, S. Chen, V.K. Ramanujan, A.J. Wolf, L. Vergnes, D.M. Ojcius, A. Rentsendorj, M. Vargas, C. Guerrero, Y. Wang, K.A. Fitzgerald, D.M. Underhill, T. Town, M. Arditi, Oxidized mitochondrial DNA activates the NLRP3 inflammasome during apoptosis, Immunity 36 (2012) 401–414.
[41] S.S. Jain, S. Paglialunga, C. Vigna, A. Ludzki, E.A. Herbst, J.S. Lally, P. Schrauwen, J. Hoeks, A.R. Tupling, A. Bonen, G.P. Holloway, High-fat diet-induced mitochondrial biogenesis is regulated by mitochondrial-derived reactive oxygen species activation of CaMKII, Diabetes 63 (2014) 1907–1913.
[42] Pancreatitis-Induced p62 Accumulation Promotes Pancreatic Cancer, Cancer Discov, 8 (2018) OF16.
[43] R. Dawra, R.P. Sah, V. Dudeja, L. Rishi, R. Talukdar, P. Garg, A.K. Saluja, Intra-acinar trypsinogen activation mediates early stages of pancreatic injury but not inflammation in mice with acute pancreatitis, Gastroenterology 141 (2011) 2210–2217 (e2212).
[44] A.S. Gukovskaya, I. Gukovsky, H. Algul, A. Habtezion, Autophagy, Inflammation, and Immune Dysfunction in the Pathogenesis of Pancreatitis, Gastroenterology 153 (2017) 1212–1226.
[45] J.H. Um, J. Yun, Emerging role of mitophagy in human diseases and physiology, BMB Rep. 50 (2017) 299–307.
[46] J. Ren, Y. Zhang, Targeting autophagy in aging and aging-related cardiovascular diseases, Trends Pharmacol. Sci. 39 (2018) 1064–1076.
[47] G. Biczo, E.T. Vegh, N. Shalbueva, O.A. Mareninova, J. Elperin, E. Lotshaw, S. Gretler, A. Lugea, S.R. Malla, D. Dawson, P. Ruchala, J. Whitelegge, S.W. French, L. Wen, S.Z. Husain, F.S. Gorelick, P. Hegyi, Z. Rakonczay Jr., I. Gukovsky, A.S. Gukovskaya, Mitochondrial dysfunction, through impaired autophagy, leads to endoplasmic reticulum stress, deregulated lipid metabolism, and pancreatitis in animal models, Gastroenterology 154 (2018) 689–703.
[48] N. Martinez-Martin, P. Maldonado, F. Gasparrini, B. Frederico, S. Aggarwal, M. Gaya, C. Tsui, M. Burbage, S.J. Keppler, B. Montaner, H.B. Jefferies, U. Nair, Y.G. Zhao, M.C. Domart, L. Collinson, A. Bruckbauer, S.A. Tooze, F.D. Batista, A switch from canonical to noncanonical autophagy shapes B cell responses, Science 355 (2017) 641–647.
[49] C.A. Shugrue, M. Alexandre, A. Diaz de Villalvilla, T.R. Kolodecik, L.H. Young, F.S. Gorelick, E.C. Thrower, Cerulein hyperstimulation decreases AMP-activated protein kinase levels at the site of maximal zymogen activation, Am. J. Physiol. Gastrointest. Liver Physiol. 303 (2012) G723–G732.
[50] E. Itakura, C. Kishi-Itakura, N. Mizushima, The hairpin-type tail-anchored SNARE syntaxin 17 targets to autophagosomes for fusion with endosomes/lysosomes, Cell 151 (2012) 1256–1269.
[51] R. Mukherjee, D.N. Criddle, A. Gukovskaya, S. Pandol, O.H. Petersen, R. Sutton, Mitochondrial injury in pancreatitis, Cell Calcium 44 (2008) 14–23.
[52] K. Palikaras, E. Lionaki, N. Tavernarakis, Balancing mitochondrial biogenesis and mitophagy to maintain energy metabolism homeostasis, Cell Death Differ. 22 (2015) 1399–1401.
[53] J. Maleth, Z. Rakonczay Jr., V. Venglovecz, N.J. Dolman, P. Hegyi, Central role of mitochondrial injury in the pathogenesis of acute pancreatitis, Acta Physiol (Oxf.) 207 (2013) 226–235.
[54] R.K. Boyapati, A. Tamborska, D.A. Dorward, G.T. Ho, Advances in the understanding of mitochondrial DNA as a pathogenic factor in inflammatory diseases, F1000Res, 6 (2017) 169.
[55] M. Bueno, D. Zank, I. Buendia-Roldan, K. Fiedler, B.G. Mays, D. Alvarez, J. Sembrat, B. Kimball, J.K. Bullock, J.L. Martin, M. Nouraie, B.A. Kaufman, M. Rojas, A. Pardo, M. Selman, A.L. Mora, PINK1 attenuates mtDNA release in alveolar epithelial cells and TLR9 mediated profibrotic responses, PLoS One 14 (2019) e0218003.
[56] S. Grazioli, J. Pugin, Mitochondrial damage-associated molecular patterns: from inflammatory signaling to human diseases, Front. Immunol. 9 (2018) 832.
[57] S.M. Jin, R.J. Youle, PINK1- and Parkin-mediated mitophagy at a glance, J. Cell Sci. 125 (2012) 795–799.
[58] C. Huang, A.M. Andres, E.P. Ratliff, G. Hernandez, P. Lee, R.A. Gottlieb, Preconditioning involves selective mitophagy mediated by Parkin and p62/SQSTM1, PLoS One 6 (2011) e20975.